

Quantum and Classical Proton Diffusion in Superconducting Clathrate Hydrides

Hui Wang^{1,*}, Yansun Yao^{2,*}, Feng Peng,³ Hanyu Liu,^{4,5,‡} and Russell J. Hemley⁶

¹Key Laboratory for Photonic and Electronic Bandgap Materials (Ministry of Education),
School of Physics and Electronic Engineering, Harbin Normal University, Harbin 150025, China

²Department of Physics and Engineering Physics, University of Saskatchewan, Saskatoon, Saskatchewan S7N 5E2, Canada

³College of Physics and Electronic Information, Luoyang Normal University, Luoyang 471022, People's Republic of China

⁴International Center for Computational Method and Software and State Key Laboratory of Superhard Materials,
College of Physics, Jilin University, Changchun 130012, China

⁵Key Laboratory of Physics and Technology for Advanced Batteries (Ministry of Education),
College of Physics and International Center of Future Science, Jilin University, Changchun 130012, China

⁶Departments of Physics and Chemistry, University of Illinois at Chicago, Chicago, Illinois 60607, USA

 (Received 20 September 2020; revised 20 November 2020; accepted 18 February 2021; published 19 March 2021)

The discovery of near room temperature superconductivity in clathrate hydrides has ignited the search for both higher temperature superconductors and deeper understanding of the underlying physical phenomena. In a conventional electron-phonon mediated picture for the superconductivity for these materials, the high critical temperatures predicted and observed can be ascribed to the low mass of the protons, but this also poses nontrivial questions associated with how the proton dynamics affect the superconductivity. Using clathrate superhydride $\text{Li}_2\text{MgH}_{16}$ as an example, we show through *ab initio* path integral simulations that proton diffusion in this system is remarkably high, with a diffusion coefficient, for example, reaching $6 \times 10^{-6} \text{ cm}^2/\text{s}$ at 300 K and 250 GPa. The diffusion is achieved primarily through proton transfer among interstitial voids within the otherwise rigid Li_2Mg sublattice at these conditions. The findings indicate the coexistence of proton quantum diffusion together with hydrogen-induced superconductivity, with implications for other very-high-temperature superconducting hydrides.

DOI: [10.1103/PhysRevLett.126.117002](https://doi.org/10.1103/PhysRevLett.126.117002)

Superconductivity at—and even above—room temperature is among the most fascinating phenomena in condensed matter physics. First suggested by early predictions for atomic metallic hydrogen [1], it is now of great interest as a result of recent breakthroughs in studies of hydrogen-rich materials under pressure. It is understood that, when a system has very high phonon vibrational frequencies, as in materials containing a great deal of hydrogen, even moderate coupling of these phonons to electron motions could result in a high superconducting T_c [1,2]. With its origins in Bardeen-Cooper-Schrieffer (BCS) theory [3], this principle has been substantiated by *ab initio* calculations and theoretical design of a large variety of H-rich hydrides [4,5] together with the experimental realization of both the predicted H-rich structures and high- T_c behavior of a growing number of H hydrides (see Refs. [6–8]). In particular, the observations of record high- T_c superconductivity of 203 K in H_3S [9] and near room temperature in LaH_{10} -based superhydride [10,11], followed by later studies of the Y-H system [12,13], have confirmed predictions [14,15]. Indeed, the T_c onset of superconductivity in a C-S-H mixture recently reported to reach room temperature at higher pressures [16] is also in accord with theoretical predictions [17,18].

In addition to electron-phonon coupling (EPC), a singular feature of both solid hydrogen [19] and H-rich

hydrides is the appreciable dynamical properties of the nuclei over a broad range of temperatures. This strong dynamics underlies predictions that compressed hydrogen could be a unique two-component system of protons and electrons exhibiting unique superconducting fluid and superconducting superfluid behavior at sufficiently high pressures [20]. Manifestations of such quantum dynamical properties are presaged in the molecular phases of dense hydrogen that have been characterized to date. For example, in the high-pressure phase IV of hydrogen, fluxional sublattice proton transfer within its graphenelike sheets of short-lived H_2 predicted by *ab initio* simulations [21] is consistent with experiment [22–24]. The phase is considered an important intermediate between molecular and atomic phases of dense solid hydrogen. Since H-rich hydrides also contain a large proportion of hydrogen, proton quantum dynamics in these materials merit investigation not considered previously, in particular, to reveal its influence on superconductivity, both predicted for pure hydrogen and now observed in superhydrides.

Clathrate hydrides are three-dimensional extended cage structures of atomic hydrogen, analogous to atomic metallic hydrogen in the atomic environment, orbital hybridization, and proposed EPC mechanism [14,15]. In some clathrate hydrides, the large cages of hydrogen are

formed by more than one crystallographic sites, e.g., H_{29} cages in YH_9 and H_{32} cages in LaH_{10} [14]. The difference in site symmetry imparts dynamical behavior of the corresponding protons, leading to potential classical and quantum diffusion between sites, analogous to the behavior of protons in hydrogen phase IV. The coexistence of appreciable proton diffusion and superconductivity in very high- T clathrate hydrides is therefore a real possibility. This scenario is reminiscent of the two-component superconducting fluid proposed for hydrogen condensates in strong magnetic fields [20]. The extent to which proton diffusion breaks or otherwise modifies the EPC in very high- T_c superconducting clathrate hydrides is thus an important question.

To address this problem and to illustrate the effect, we focused on Li_2MgH_{16} [25] as a model system because of its very high predicted T_c based on the theoretical schemes that led to discoveries of high- T_c hydrides H_3S and LaH_{10} and the Y-H superconductors. In Li_2MgH_{16} , the hydrogen atoms form a clathrate framework consisting of face-shared H_{28} cages with nearest H-H distances of 1.02–1.23 Å at 250–300 GPa (Fig. 1). At these pressures, this material is calculated to have very high T_c 's with a large variation (330–473 K), which provides a wide P - T range for exploring the classical and quantum proton diffusion and its effects on superconductivity in the clathrate H framework. In Li_2MgH_{16} , the Li and Mg atoms are arranged in a C15 cubic Laves sublattice in which the Mg atoms form a diamond structure with the four tetrahedral voids occupied by Li tetrahedra. All interstitial sites in this sublattice are tetrahedral and thus grouped in g , e , and b Wyckoff sites and coordinated by $[Li_2Mg_2]$, $[Li_3Mg]$, and $[Li_4]$ tetrahedra, respectively (Fig. 1). Notably, unusual proton dynamics in isolated hexagons formed by nearest g sites has been documented experimentally in C15-Laves hydride solutions [26,27]. Localized hopping of protons within single hexagons was found at low temperatures (as low as

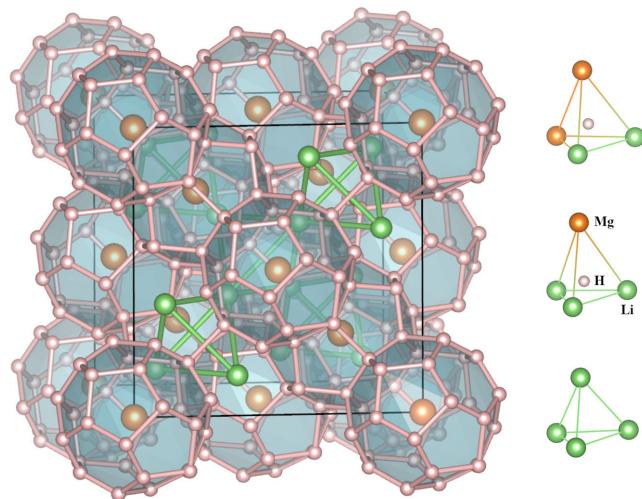


FIG. 1. Clathrate structure of Li_2MgH_{16} (space group $Fd\bar{3}m$).

30 K), but at room temperature, the proton motion evolves toward long-range diffusion across neighboring hexagons. In Li_2MgH_{16} , the clathrate H framework has fully occupied g and e sites, whereas the b sites are empty; therefore, different proton dynamics is expected.

To further probe the proton motion in Li_2MgH_{16} , we derived the occupation numbers of the g , e , and b sites at different temperatures from NVT molecular dynamics (MD) trajectories of 2 ps at 20 fs intervals at 250 and 300 GPa [Figs. 2(a) and 2(b); see Supplemental Material [28] for details]. At 250 GPa, a moderate g - b redistribution of proton density is seen at all temperatures at the beginning of the trajectory. This process appears to be intrinsic; i.e., the g tetrahedra are sufficiently large that even zero-point vibrations can set off the enclosed protons and transfer them to empty sites in the structure. In contrast, at 300 GPa, the g - b redistribution occurs only at temperatures above 25 K, indicating that the g tetrahedra are now reduced and hold the protons more tightly, so only those with sufficient kinetic energy can break through. The e site is midway between the g and b sites and therefore acts as a channel for the g - b redistribution, which explains the simultaneous fluctuation of occupation of the e sites with the redistribution. Thermal motion destabilizes the tetrahedral enclosure of protons, especially for those at the g sites being least constrained by the $[Li_2Mg_2]$ tetrahedra.

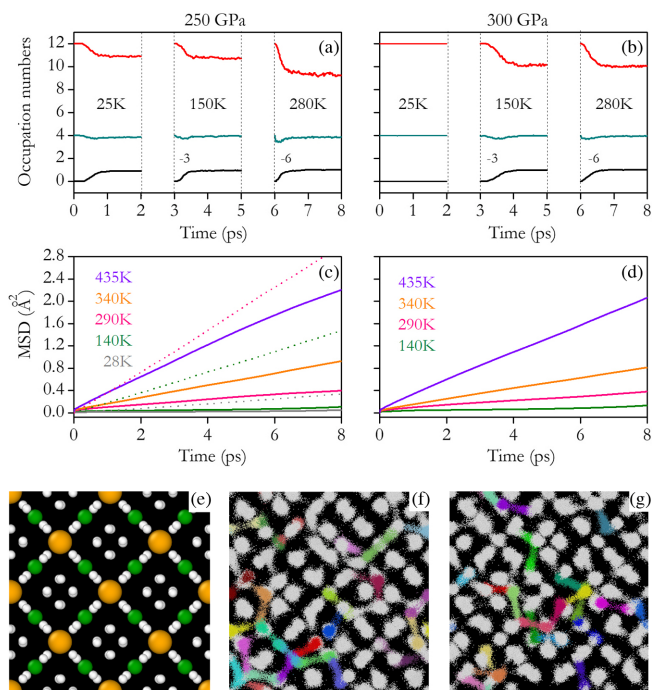


FIG. 2. (a),(b) Occupation numbers of g (red), e (cyan), and b (black) sites. (c),(d) The MSD of the H component of Li_2MgH_{16} from MD (solid) at 28–435 K and RPMD (dotted) at 300 K (pink), 150 K (green), and 30 K (gray). (e) The $[100]$ view of Li_2MgH_{16} . (f),(g) Proton density distributions at ~ 30 K and 250–300 GPa calculated from PIMD with 16 beads in the cubic cell of 152 atoms; selected protons are marked by different colors.

The mean square displacement (MSD) curves of the hydrogens derived from longer *NPT* MD trajectories are shown in Figs. 2(c) and 2(d) [28]. At 250 GPa and 25 K, proton diffusion other than *g-b* redistribution is rare, as shown by the almost flat gray curve. At higher temperatures, nonlocal proton motions become obvious, as revealed in the progressive increase of the MSD slope. At 300 GPa, the temperature-induced increase in MSD follows the same trend but with smaller values due to the more restricted proton motion in the structure. The average diffusion coefficient between 250 and 300 GPa at 140 K obtained from these curves is 2.4×10^{-7} cm²/s, which is remarkably the same order of magnitude as that measured for C15-Laves hydride solutions TaV₂H_{*x*} (*x* = 0.6 and 1.1) at ambient conditions [27]. This agreement can be understood by recognizing that the proton diffusion is equivalent to void diffusion moving in the opposite direction, analogous to the electron-hole equivalence in semiconductors, and the number of empty tetrahedral voids in a Li₂MgH₁₆ formula unit is comparable to that of hydrogen sites in TaV₂H_{*x*} solutions. With increasing temperature, the calculated average diffusion coefficient increases to 1.0×10^{-6} cm²/s at 290 K and 4.4×10^{-6} cm²/s at 435 K.

To explore the nuclear quantum effects, we performed path integral molecular dynamics (PIMD) simulations [35] on Li₂MgH₁₆. It is clearly seen that the proton is quantum diffusive at 30 K and both 250 and 300 GPa [Figs. 2(f) and 2(g)], despite neglecting nuclear exchange. Proton density distributions between neighboring hexagons suggest that the diffusion is nonlocal even at low temperature. Further ring polymer molecular dynamics (RPMD) gave average diffusion coefficients of 7.1×10^{-7} , 3.1×10^{-6} , and 6.3×10^{-6} cm²/s at 30, 150, and 300 K, respectively. The appreciable values indicate that this robust quantum diffusion persists to high temperatures. On the other hand, the values are a factor $\sim 10^2$ lower than the criterion for classical superionicity ($\sim 10^{-4}$ cm²/s), i.e., with protons diffusing freely within the structure [45]. The result suggests that proton diffusion is not strong enough to significantly change the statistical distribution of vibrational (or electronic) density of states predicted for Li₂MgH₁₆.

The atomic configurations of Li₂MgH₁₆ were characterized by the average radial distribution function [RDF, *g*(*r*)] as shown in Fig. 3(a) for at 250 GPa and 290 K. Atomic vibrations eliminate the small gaps among the nearest inter- and intrahexagon *g-g*, *g-e*, and *e-b* separations of the initial structure, resulting in the formation of the first coordination shell of H peaked at ~ 1.1 Å, which nearly coincides with that found for LaH₁₀ at comparable conditions (190 GPa and 240 K). The position of this peak is almost unchanged with temperature from 140 to 435 K, but it shifts down to ~ 1.07 Å at 300 GPa. Comparing the RDFs in the Li₂Mg sublattice to those for La in LaH₁₀ (Supplemental Material, Fig. S9 [28]) reveals that increased external pressure can compensate for the lower degree of

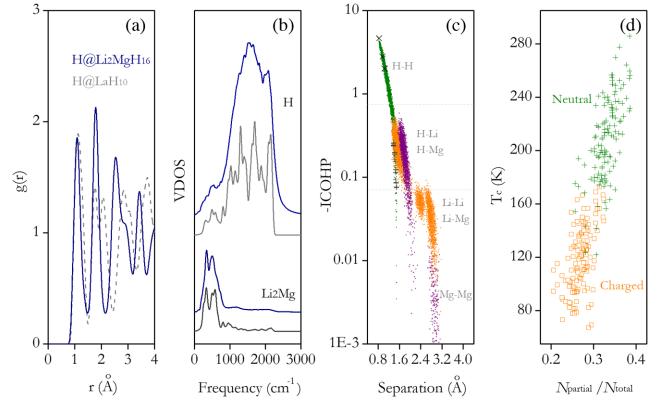


FIG. 3. (a) The *g*(*r*) of the H framework of Li₂MgH₁₆ at 250 GPa and 290 K compared to that of LaH₁₀ at 190 GPa and 240 K. (b) VDOS of Li₂MgH₁₆ at 290 K (blue) and 0 K (gray) at that pressure. (c) The *I* as a function of pair separations at 250 GPa and 290 K. (d) Configurationally distinguished *T_c* as a function of the ratio of partial to total *N*(*ε_F*) of the H framework at 250–300 GPa and 140–290 K.

“precompression” by smaller ions on condensing the H framework. Notably, proton diffusion in the Li₂Mg sublattice occurs at a much lower temperature than in the La sublattice of LaH₁₀ (~ 800 K) [46]. This difference arises from the more flexible sublattice of interstitial sites of light elements and unsaturated occupation of those sites in Li₂MgH₁₆.

The vibrational density of states (VDOS) was calculated from the Fourier transform of the velocity autocorrelation functions [24], as shown in Fig. 3(b) for the 290 K and 250 GPa simulations. Proton diffusion results in a small but nonzero VDOS of H at zero frequency, with the value about 3% of the peak at 1563 cm⁻¹, which is consistent with the small diffusion coefficients. The bonding interactions between neighboring atoms were also evaluated by the negative of crystal orbital Hamiltonian population (COHP) integrals at the Fermi level *ε_F* (denoted as *I*) [36]. We take the value of *I* for the H-H contact within the graphenelike layer (*I_l*) and that between two adjacent layers (*I_{ll}*) using the *oP48* structure for hydrogen phase IV at 0 K and 250 GPa as a strength measure [21]. The results indicate that the interactions in Li₂MgH₁₆ at 290 K and 250 GPa can be roughly divided into three regions: $< I_{ll}$, $\sim I_{ll}$, and $\sim I_l$ [Fig. 3(c)]. The *I* values for H-H interactions cover all three regions, in line with the diverse motion behavior of protons and associated broad range of vibrational frequencies in the material.

The fluxional or diffusive nature of the H framework in these clathrate hydride structures have implications for calculations of their superconducting properties. As a first step in examining this, we estimated within a BCS framework the EPC constant *λ* for the H component of Li₂MgH₁₆, either neutral or charged with $0.25 e^-/H$ (see Supplemental Material [28] for details). The configurationally averaged

λ fall in a range of 1.0–1.1 and 1.5–1.6 for the charged and neutral H frameworks, respectively. Although these values indicate strong EPC, they are smaller than that predicted for cubic LaH₁₀ (1.78–2.29) in the same pressure range at 0 K [14]. Assuming $\mu^* = 0.1$ –0.13, configurationally averaged T_c 's of 110–148 and 176–245 K were obtained from the Allen-Dynes equation [44] for the charged and neutral H frameworks, respectively [Fig. 3(d)]. These estimated T_c 's are below those predicted for the “static,” nondiffusive structures (330–473 K) obtained by solving the Eliashberg equation (at 0 K) [25], but they still extend to high temperatures and span the range over which we find strong classical and quantum diffusion. As discussed before, proton diffusion is not strong enough to significantly change the statistical distribution values of vibrational-electronic density of states, indicating that the Hopfield parameter calculated from *NPT* configurations could give a reasonable estimation on λ and T_c , even without considering quantum diffusion.

Quantum and classical diffusion may occur in other superconducting superhydrides systems below T_c . Further simulations of coupled quantum diffusion and superconductivity, including the effect of the strong quantum behavior on pairing going well beyond BCS and other conventional models, are required in order to obtain accurate predictions of superconducting critical temperatures for these materials [20,47]. As such, clathrate superhydrides, which contain a dense atomic hydrogen sublattice similar to that of atomic metallic hydrogen, provide a testable model for this behavior, as indicated by very recent results pointing to possible T_c well above room temperatures [48]. The anticipated new phenomena invite continued experimental investigations that will advance our understanding of this novel class of quantum materials.

H. W. is thankful to Y. Ma and M. Shiga for valuable discussions. This work was supported by the National Natural Science Foundation of China (Grants No. 11974135, No. 11874176, No. 11774140, No. 11874175, No. 11974134, and No. 12074138), the Natural Sciences and Engineering Research Council of Canada, the China Postdoctoral Science Foundation under Grant No. 2016M590033, the Program for JLUSTIRT, and U.S. National Science Foundation (DMR-1933622; R. J. H.). We used the computing facilities at the High-Performance Computing Centre of Jilin University and Beijing Super Cloud Computing Center.

*H. W. and Y. Y. contributed equally to this work.

[†]wh@fysik.cn

[‡]hanyuliu@jlu.edu.cn

- [1] N. W. Ashcroft, *Phys. Rev. Lett.* **21**, 1748 (1968).
 [2] N. W. Ashcroft, *Phys. Rev. Lett.* **92**, 187002 (2004).
 [3] J. Bardeen, L. N. Cooper, and J. R. Schrieffer, *Phys. Rev.* **108**, 1175 (1957).

- [4] L. Zhang, Y. Wang, J. Lv, and Y. Ma, *Nat. Rev. Mater.* **2**, 17005 (2017).
 [5] A. R. Oganov, C. J. Pickard, Q. Zhu, and R. J. Needs, *Nat. Rev. Mater.* **4**, 331 (2019).
 [6] T. Bi, N. Zarifi, T. Terpstra, and E. Zurek, *Reference Module in Chemistry, Molecular Sciences and Chemical Engineering* (Elsevier, New York, 2019).
 [7] C. J. Pickard, I. Errea, and M. I. Eremets, *Annu. Rev. Condens. Matter Phys.* **11**, 57 (2020).
 [8] J. A. Flores-Livas, L. Boeri, A. Sanna, G. Profeta, R. Arita, and M. Eremets, *Phys. Rep.* **856**, 1 (2020).
 [9] A. P. Drozdov, M. I. Eremets, I. A. Troyan, V. Ksenofontov, and S. I. Shylin, *Nature (London)* **525**, 73 (2015).
 [10] M. Somayazulu, M. Ahart, A. K. Mishra, Z. M. Geballe, M. Baldini, Y. Meng, V. V. Struzhkin, and R. J. Hemley, *Phys. Rev. Lett.* **122**, 027001 (2019).
 [11] A. P. Drozdov *et al.*, *Nature (London)* **569**, 528 (2019).
 [12] P. P. Kong *et al.*, arXiv:1909.10482v1.
 [13] I. A. Troyan *et al.*, arXiv:1908.01534.
 [14] H. Liu, I. I. Naumov, R. Hoffmann, N. W. Ashcroft, and R. J. Hemley, *Proc. Natl. Acad. Sci. U.S.A.* **114**, 6990 (2017).
 [15] F. Peng, Y. Sun, C. J. Pickard, R. J. Needs, Q. Wu, and Y. Ma, *Phys. Rev. Lett.* **119**, 107001 (2017).
 [16] E. Snider, N. Dasenbrock-Gammon, R. McBride, M. Debessai, H. Vindana, K. Venkatasamy, K. V. Lawler, A. Salamat, and R. P. Dias, *Nature (London)* **586**, 373 (2020).
 [17] W. Cui, T. Bi, J. Shi, Y. Li, H. Liu, E. Zurek, and R. J. Hemley, *Phys. Rev. B* **101**, 134504 (2020).
 [18] Y. Sun, Y. Tian, B. Jiang, X. Li, H. Li, T. Iitaka, X. Zhong, and Y. Xie, *Phys. Rev. B* **101**, 174102 (2020).
 [19] H.-k. Mao and R. J. Hemley, *Rev. Mod. Phys.* **66**, 671 (1994).
 [20] E. Babaev, A. Sudbø, and N. W. Ashcroft, *Nature (London)* **431**, 666 (2004).
 [21] H. Liu and Y. Ma, *Phys. Rev. Lett.* **110**, 025903 (2013).
 [22] R. P. Dias, O. Noked, and I. F. Silvera, *Phys. Rev. Lett.* **116**, 145501 (2016).
 [23] A. F. Goncharov, I. Chuvashova, C. Ji, and H.-k. Mao, *Proc. Natl. Acad. Sci. U.S.A.* **116**, 25512 (2019).
 [24] C. S. Zha, Z. Liu, M. Ahart, R. Boehler, and R. J. Hemley, *Phys. Rev. Lett.* **110**, 217402 (2013).
 [25] Y. Sun, J. Lv, Y. Xie, H. Liu, and Y. Ma, *Phys. Rev. Lett.* **123**, 097001 (2019).
 [26] A. V. Skripov, J. C. Cook, D. S. Sibirtsev, C. Karmonik, and R. Hempelmann, *J. Phys. Condens. Matter* **10**, 1787 (1998).
 [27] A. V. Skripov, *J. Alloys Compd.* **404–406**, 224 (2005).
 [28] See Supplemental Material at <http://link.aps.org/supplemental/10.1103/PhysRevLett.126.117002> for computational details, MSD, VDOS, and EDOS, which includes Refs. [29–44].
 [29] G. Kresse and J. Furthmüller, *Phys. Rev. B* **54**, 11169 (1996).
 [30] P. E. Blöchl, *Phys. Rev. B* **50**, 17953 (1994).
 [31] J. P. Perdew, K. Burke, and M. Ernzerhof, *Phys. Rev. Lett.* **77**, 3865 (1996).
 [32] R. P. Feynman, *Statistical Mechanics: A Set of Lectures* (Hachette, UK, 1998).
 [33] A. R. H. R. P. Feynman and D. F. Styer, *Quantum Mechanics and Path Integrals* (Courier Corporation, New York, 2010).
 [34] S. Ruiz-Barragan, K. Ishimura, and M. Shiga, *Chem. Phys. Lett.* **646**, 130 (2016).

- [35] M. Shiga, *Reference Module in Chemistry, Molecular Sciences and Chemical Engineering* (Elsevier, New York, 2018).
- [36] R. Dronskowski and P. E. Bloechl, *J. Phys. Chem.* **97**, 8617 (1993).
- [37] K. Momma and F. Izumi, *J. Appl. Crystallogr.* **44**, 1272 (2011).
- [38] A. Stukowski, *Model. Simul. Mater. Sci. Eng.* **18**, 015012 (2010).
- [39] S. Le Roux and P. Jund, *Comput. Mater. Sci.* **49**, 70 (2010).
- [40] W. L. McMillan, *Phys. Rev.* **167**, 331 (1968).
- [41] J. J. Hopfield, *Phys. Rev.* **186**, 443 (1969).
- [42] G. D. Gaspari and B. L. Gyorffy, *Phys. Rev. Lett.* **28**, 801 (1972).
- [43] P. Blaha, K. Schwarz, P. Sorantin, and S. B. Trickey, *Comput. Phys. Commun.* **59**, 399 (1990).
- [44] P. B. Allen and R. C. Dynes, *Phys. Rev. B* **12**, 905 (1975).
- [45] E. Katoh, H. Yamawaki, H. Fujihisa, M. Sakashita, and K. Aoki, *Science* **295**, 1264 (2002).
- [46] H. Liu, I. I. Naumov, Z. M. Geballe, M. Somayazulu, J. S. Tse, and R. J. Hemley, *Phys. Rev. B* **98**, 100102(R) (2018).
- [47] M. Y. Kagan and A. Bianconi, *Condens. Matter* **4**, 51 (2019).
- [48] A. D. Grockowiak *et al.*, arXiv:2006.03004.